

Generalized polarizabilities of the nucleon studied in the linear sigma model (II)

A. Metz and D. Drechsel

*Institut für Kernphysik, Johannes Gutenberg-Universität Mainz, J. J. Becher-Weg 45, D-55099
Mainz, Germany*

(October 7, 2018)

Abstract

In a previous paper virtual Compton scattering off the nucleon has been investigated in the one-loop approximation of the linear sigma model in order to determine the 3 scalar generalized polarizabilities. We have now extended this work and calculated the 7 vector polarizabilities showing up in the spin-dependent amplitude of virtual Compton scattering. The results fulfill 3 model-independent constraints recently derived. Compared to the constituent quark model there exist enormous differences for some of the vector polarizabilities. At vanishing three-momentum of the virtual photon, the analytical results of the sigma model and of chiral perturbation theory can be related. The influence of the π^0 exchange in the t channel has been discussed in some detail. Besides, the vector polarizabilities determine 2 linear combinations of the third order spin-polarizabilities appearing in real Compton scattering.

12.39.Fe, 13.60.Fz

I. INTRODUCTION

Recently, it has been proposed to study the structure of the proton by the reaction $p(e, e'p)\gamma$. The reason is that this process contains, in addition to electron bremsstrahlung (Bethe–Heitler scattering), the amplitude of virtual Compton scattering (VCS) off the proton, $\gamma^* + p \rightarrow \gamma + p$. In general, Compton scattering as a two step process allows to extract information on the excitation spectrum of the target.

An overview of the various aspects of VCS can be found in Ref. [1]. VCS is of particular interest below pion production threshold, where the information about the excited states of the nucleon can be parametrized by means of the generalized electromagnetic polarizabilities. These generalized polarizabilities emerge as coefficients if the non Born amplitude of VCS is expanded in terms of the final photon energy $\omega' = 0$. As has been demonstrated by Guichon et al. [2], the leading term of such an expansion contains 10 generalized polarizabilities, 3 of them in the spin-independent amplitude (scalar polarizabilities) and 7 in the spin-flip amplitude (vector polarizabilities). In contrast to real Compton scattering (RCS), the generalized polarizabilities in VCS are functions depending on the four-momentum transfer Q^2 .

At present, three experimental programs are under way to determine the generalized polarizabilities. At MAMI, data have been taken at $Q^2 = 0.33 \text{ GeV}^2$ [3]. There also exist plans to investigate VCS at even lower values of Q^2 at MIT–Bates [4], while the activities at Jefferson Lab will concentrate on the region of higher Q^2 [5]. In an unpolarized experiment only 3 independent linear combinations of the polarizabilities can be determined [2,10]. A separate measurement of all polarizabilities is only possible by use of double polarization observables, e.g., the reaction $p(\vec{e}, e'\vec{p})\gamma$ [7]. Moreover, a careful treatment of radiative corrections is unavoidable as their contributions are comparable to the polarizability effects [8].

Regarding the expansion in ω' for RCS, higher order terms can not be neglected at photon energies larger than about 80 MeV. In order to guarantee the dominance of the leading order term, the energy of the real photon should also satisfy $\omega' \ll E - m_N$, where E is the energy of the initial nucleon in the cm system and m_N the nucleon mass [6], i.e., ω' has to be much smaller than the three-momentum $|\vec{q}|$ of the virtual photon (see section II). If ω' and $|\vec{q}|$ are of the same order of magnitude, the amplitude has to be expanded in both variables (see Ref. [9] for the case of a spin 0 target). The extension of this work to the nucleon leads to 36 independent low energy constants entering the non-Born VCS amplitude to fifth order [10]. While it is certainly hopeless to measure these parameters, we want to emphasize the importance of a reliable estimate of the higher order terms, except for very small values of ω' .

Recently, it has been shown that the combined symmetry of charge conjugation and nucleon crossing results in unexpected relations between the VCS multipoles, beyond the usual constraints of parity and angular momentum conservation [6,10]. As a consequence, only 2 independent scalar and 4 independent vector polarizabilities exist.

The generalized polarizabilities of the proton were first predicted by use of the constituent quark model (CQM) [2,11]. Further calculations in an effective Lagrangian model [12], the linear sigma model (LSM) [13], chiral perturbation theory (ChPT) [14,15], and the Skyrme model [16] focused on the scalar polarizabilities and the spin-independent VCS amplitude.

In the meantime, the vector polarizabilities have been evaluated on the basis of ChPT [17,18] and in a coupled-channel unitary model [19].

The present contribution completes our earlier work on the LSM [13] by presenting the results for the vector polarizabilities. Since the model is chirally invariant, we expect similar results as in ChPT for $Q^2 \rightarrow 0$, and in addition a reasonable estimate for the Q^2 dependence of the polarizabilities.

II. KINEMATICS

For convenience we briefly repeat the definition of the kinematical variables for the VCS reaction [13,20]

$$\gamma^*(q^\mu, \varepsilon^\mu) + N(p^\mu, S^\mu) \rightarrow \gamma(q'^\mu, \varepsilon'^\mu) + N'(p'^\mu, S'^\mu), \quad \text{with } q^2 = -Q^2 < 0, \quad q'^2 = 0. \quad (1)$$

The *cm* energies and three-momenta of the involved particles are denoted by $q^\mu = (\omega, \vec{q})$, $q'^\mu = (\omega', \vec{q}')$, $p^\mu = (E, -\vec{q})$, $p'^\mu = (E', -\vec{q}')$. The polarization vectors of both photons can be chosen to be spacelike, i.e., $\varepsilon^\mu = (0, \vec{\varepsilon})$ and $\varepsilon'^\mu = (0, \vec{\varepsilon}')$, noting that the time-like component of the virtual photon can be eliminated by current conservation. While the outgoing photon is purely transverse (helicity $\lambda = \pm 1$), the incoming photon has also longitudinal polarization ($\lambda = 0$), denoted by $\varepsilon^\mu(\lambda = 0) = (0, \hat{q})$. In the following we also use the definitions

$$\omega_0 = \omega|_{\omega'=0} = m_N - E = m_N - \sqrt{\vec{q}^2 + m_N^2}, \quad (2)$$

$$Q_0^2 = Q^2|_{\omega'=0} = -2m_N\omega_0, \quad (3)$$

with $\bar{q} \equiv |\vec{q}|$.

With the convention of Bjorken and Drell [21] for the invariant matrix element \mathcal{M} we define the scattering amplitude T by

$$T = -\frac{i}{4\pi} \mathcal{M} = -\frac{i}{4\pi} \varepsilon'^{\mu*} H^{\mu\nu} \varepsilon_\nu. \quad (4)$$

As the Compton tensor $H^{\mu\nu}$ consists of 12 basis elements [22,10], T can be decomposed into 12 independent amplitudes. Following Guichon et al. [2], we parametrize the longitudinal and the transverse part of T in Pauli space,

$$T(\lambda = 0) = \chi_f^\dagger [\vec{\varepsilon}'^* \cdot \hat{q} a^l + i \vec{\varepsilon}'^* \cdot (\hat{q} \times \hat{q}') \vec{\sigma} \cdot \hat{e}_x b_1^l + i \vec{\varepsilon}'^* \cdot \hat{q} \vec{\sigma} \cdot \hat{e}_y b_2^l + i \vec{\varepsilon}'^* \cdot (\hat{q} \times \hat{q}') \vec{\sigma} \cdot \hat{e}_z b_3^l] \chi_i, \quad (5)$$

$$T(\lambda = \pm 1) = \chi_f^\dagger [\vec{\varepsilon}'^* \cdot \vec{\varepsilon} a^t + \vec{\varepsilon}'^* \cdot \hat{q} \vec{\varepsilon} \cdot \hat{q}' a^{t'} + i \vec{\varepsilon}'^* \cdot \hat{q} \vec{\varepsilon} \cdot (\hat{q} \times \hat{q}') \vec{\sigma} \cdot \hat{e}_x b_1^t + i \vec{\varepsilon}'^* \cdot \hat{q}' \vec{\varepsilon}'^* \cdot (\hat{q} \times \hat{q}') \vec{\sigma} \cdot \hat{e}_x b_1^{t'} + i \vec{\varepsilon}'^* \cdot \vec{\varepsilon} \vec{\sigma} \cdot \hat{e}_y b_2^t + i \vec{\varepsilon}'^* \cdot \hat{q} \vec{\varepsilon} \cdot \hat{q}' \vec{\sigma} \cdot \hat{e}_y b_2^{t'} + i \vec{\varepsilon}'^* \cdot \hat{q} \vec{\varepsilon} \cdot (\hat{q} \times \hat{q}') \vec{\sigma} \cdot \hat{e}_z b_3^t + i \vec{\varepsilon}'^* \cdot \hat{q}' \vec{\varepsilon}'^* \cdot (\hat{q} \times \hat{q}') \vec{\sigma} \cdot \hat{e}_z b_3^{t'}] \chi_i, \quad (6)$$

where χ_i and χ_f are the Pauli spinors of the nucleon. There appear 3 spin-independent and 9 spin-dependent amplitudes as functions of 3 variables, e.g., the covariants q^2 , $q \cdot q'$ and

$q \cdot p$. In the following we will use an equivalent, non-covariant set of arguments, ω' , \bar{q} and $\cos \vartheta = \hat{q} \cdot \hat{q}'$. The orthonormal coordinate system

$$\hat{e}_x = \frac{\hat{q}' - \cos \vartheta \hat{q}}{\sin \vartheta}, \quad \hat{e}_y = \frac{\hat{q} \times \hat{q}'}{\sin \vartheta}, \quad \hat{e}_z = \hat{q} \quad (7)$$

is fixed by the momenta of the photons.

III. GENERALIZED POLARIZABILITIES

The scattering amplitude is decomposed into the Born contribution T_B and the non-Born or residual contribution T_R ,

$$T = T_B + T_R, \quad (8)$$

and the generalized polarizabilities are given by a low energy expansion of T_R with respect to ω' [2]. As has been pointed out in Refs. [2,23], the splitting in (8) is not unique. Contributions which are regular in the limit $\omega' \rightarrow 0$ and separately gauge invariant can be shifted from the Born amplitude to the residual amplitude and vice versa. Therefore, when calculating the generalized polarizabilities, one has to specify which Born terms have been subtracted from the full amplitude, since different Born terms lead to different numerical values of the polarizabilities. In our calculation we use the Born amplitude as defined in [13].

To be specific, the generalized polarizabilities have been derived from the multipoles $H_R^{(\rho'L',\rho L)S}(\omega', \bar{q})$ of the residual amplitude [2]. In this notation ρ (ρ') represents the charge (0), magnetic (1) or electric (2) nature of the initial (final) photon, while L (L') refers to its angular momentum. The quantum number S characterizes the no spin-flip ($S = 0$) and the spin-flip ($S = 1$) transitions.

For the definition of the generalized polarizabilities it is necessary to know the low energy behaviour of the multipoles if $(\omega', \bar{q}) \rightarrow (0, 0)$. While the Coulomb and the magnetic transitions are well behaved in that limit, the electric transitions of the virtual photon depend on the path along which the origin in the ω' - \bar{q} -plane is approached. Since we are only interested in the leading order term in $|\vec{q}'| = \omega'$, we can express the electric transitions of the outgoing photon by the Coulomb transitions [2],

$$H_R^{(2L',\rho L)S}(\omega', \bar{q}) = -\sqrt{\frac{L'+1}{L'}} H_R^{(0L',\rho L)S}(\omega', \bar{q}) + \mathcal{O}(\omega'^{L'+1}). \quad (9)$$

The corresponding equation for the incoming photon reads

$$H_R^{(\rho'L',2L)S}(\omega', \bar{q}) = -\sqrt{\frac{L+1}{L}} \frac{\omega}{\bar{q}} H_R^{(\rho'L',0L)S}(\omega', \bar{q}) - \sqrt{\frac{2L+1}{L}} \hat{H}_R^{(\rho'L',L)S}(\omega', \bar{q}). \quad (10)$$

Note that no expansion in the three-momentum \bar{q} of the virtual photon is performed. Hence, one has to keep the difference $\hat{H}_R^{(\rho'L',L)S}$ between the electric and the charge multipoles. Even if this difference has a mixed multipole character, it has an obvious and path-independent low energy behaviour [2].

The generalized polarizabilities are defined according to [2] as

$$P^{(\rho'L',\rho L)S}(\bar{q}) = \left[\frac{1}{\omega'^{L'}\bar{q}^L} H_R^{(\rho'L',\rho L)S}(\omega', \bar{q}) \right]_{\omega'=0} \quad (\rho, \rho' = 0, 1), \quad (11)$$

$$\hat{P}^{(\rho'L',L)S}(\bar{q}) = \left[\frac{1}{\omega'^{L'}\bar{q}^{L+1}} \hat{H}_R^{(\rho'L',L)S}(\omega', \bar{q}) \right]_{\omega'=0} \quad (\rho' = 0, 1). \quad (12)$$

In the following we restrict ourselves to electric and magnetic dipole transitions of the real photon, which is equivalent to keep only the leading, linear term in ω' of the residual amplitude T_R . In that case there exist, due to conservation of parity and angular momentum, 3 scalar multipoles ($S = 0$) and 7 vector multipoles ($S = 1$).

To evaluate the vector polarizabilities it is sufficient to treat the following 5 out of the 9 spin-dependent amplitudes of eqs. (5) and (6):

$$b_{R,1}^l = \frac{e^2}{4\pi} \sqrt{\frac{E}{m_N}} \frac{\omega'}{\sin \vartheta} \frac{\sqrt{3}}{2} \left[\frac{\omega_0}{\bar{q}} \cos \vartheta \left(P^{(11,00)1} + \frac{\bar{q}^2}{\sqrt{2}} P^{(11,02)1} \right) - \sqrt{3} \omega_0 P^{(01,01)1} \right] + \mathcal{O}(\omega'^2), \quad (13)$$

$$b_{R,3}^l = \frac{e^2}{4\pi} \sqrt{\frac{E}{m_N}} \omega' \frac{\sqrt{3}}{2} \left[\frac{\omega_0}{\bar{q}} \left(-P^{(11,00)1} + \sqrt{2} \bar{q}^2 P^{(11,02)1} \right) \right] + \mathcal{O}(\omega'^2), \quad (14)$$

$$b_{R,1}^t = \frac{e^2}{4\pi} \sqrt{\frac{E}{m_N}} \frac{\omega'}{\sin \vartheta} \frac{3}{4} \left[2\omega_0 P^{(01,01)1} + \sqrt{2} \bar{q}^2 \left(P^{(01,12)1} + \sqrt{3} \hat{P}^{(01,1)1} \right) \right] + \mathcal{O}(\omega'^2), \quad (15)$$

$$b_{R,1}^{t'} = \frac{e^2}{4\pi} \sqrt{\frac{E}{m_N}} \frac{\omega'}{\sin \vartheta} \frac{3}{4} \left[\bar{q} P^{(11,11)1} + \frac{\sqrt{3}}{\sqrt{2}} \omega_0 \bar{q} P^{(11,02)1} + \frac{\sqrt{5}}{\sqrt{2}} \bar{q}^3 \hat{P}^{(11,2)1} \right] + \mathcal{O}(\omega'^2), \quad (16)$$

$$b_{R,3}^{t'} = \frac{e^2}{4\pi} \sqrt{\frac{E}{m_N}} \frac{\omega'}{\sin^2 \vartheta} \frac{3}{4} \left[2\omega_0 P^{(01,01)1} + \sqrt{2} \bar{q}^2 \left(-P^{(01,12)1} + \sqrt{3} \hat{P}^{(01,1)1} \right) \right. \\ \left. + \cos \vartheta \left(\bar{q} P^{(11,11)1} - \frac{\sqrt{3}}{\sqrt{2}} \omega_0 \bar{q} P^{(11,02)1} - \frac{\sqrt{5}}{\sqrt{2}} \bar{q}^3 \hat{P}^{(11,2)1} \right) \right] + \mathcal{O}(\omega'^2). \quad (17)$$

Because of their angular dependence, $b_{R,1}^l$ and $b_{R,3}^{t'}$ contain two independent linear combinations of the polarizabilities.

Based upon gauge invariance, Lorentz invariance, parity conservation, and charge conjugation in connection with nucleon crossing, it was shown in Ref. [10] that only four independent vector polarizabilities exist. This fact is reflected by the equations

$$0 = P^{(11,11)1}(\bar{q}) + \sqrt{\frac{3}{2}} \omega_0 P^{(11,02)1}(\bar{q}) + \sqrt{\frac{5}{2}} \bar{q}^2 \hat{P}^{(11,2)1}(\bar{q}), \quad (18)$$

$$0 = 2\omega_0 P^{(01,01)1}(\bar{q}) + 2\frac{\bar{q}^2}{\omega_0} P^{(11,11)1}(\bar{q}) - \sqrt{2} \bar{q}^2 P^{(01,12)1}(\bar{q}) + \sqrt{6} \bar{q}^2 \hat{P}^{(01,1)1}(\bar{q}), \quad (19)$$

$$0 = 3\frac{\bar{q}^2}{\omega_0} P^{(01,01)1}(\bar{q}) - \sqrt{3} P^{(11,00)1}(\bar{q}) - \sqrt{\frac{3}{2}} \bar{q}^2 P^{(11,02)1}(\bar{q}). \quad (20)$$

Due to (18) the amplitude $b_{R,1}^{t'}$ vanishes to linear order in ω' . Equations (19,20) relate the angular-independent and the angular-dependent terms of $b_{R,1}^l$ and $b_{R,3}^{t'}$. Moreover, the relations

$$P^{(01,01)1}(0) = P^{(11,11)1}(0) = P^{(11,00)1}(0) = 0 \quad (21)$$

have been established [10]. At $\bar{q} = 0$, further specific relations between the polarizabilities and their derivatives can be obtained by expanding (18)–(20) with respect to Q_0^2 or \bar{q}^2 . We have used such expansions up to Q_0^4 in order to test our analytical results. Furthermore we note that the polarizabilities are actually functions of \bar{q}^2 [10].

Equivalent to the parametrization of the spin–flip amplitude of VCS in terms of generalized vector polarizabilities, Ragusa [24] expressed the spin–flip amplitude in RCS, to lowest order in the photon energy, by 4 polarizabilities, called $\gamma_1, \gamma_2, \gamma_3, \gamma_4$. Two linear combinations of these γ_i can be related to the generalized polarizabilities [10],

$$\gamma_3 = -\frac{e^2}{4\pi} \frac{3}{\sqrt{2}} P^{(01,12)1}(0), \quad \gamma_2 + \gamma_4 = -\frac{e^2}{4\pi} \frac{3\sqrt{3}}{2\sqrt{2}} P^{(11,02)1}(0). \quad (22)$$

To recover the remaining two combinations of Ragusa, one has to go beyond the leading order term in ω' . We note that the right hand sides of (22) are not unique, because of the relations between the generalized polarizabilities.

IV. RESULTS AND DISCUSSION

The one–loop diagrams contributing to the generalized polarizabilities in the LSM for infinite sigma mass were shown in [13]. While the sigma exchange in the t channel strongly influences the numerical values of the scalar polarizabilities α and β , it does not contribute to the vector polarizabilities. On the other hand, the π^0 exchange in the t channel (anomaly, see Fig. 1) is irrelevant in the spin–independent case, but very important for calculations of the vector polarizabilities. Since the anomaly is gauge invariant and regular in the soft photon limit, it could also be considered as part of the Born amplitude [2]. Our results without the anomaly are discussed in the following subsection A, and the anomaly is treated in subsection B.

A. Numerical results

Figure 2 displays our numerical results for the 7 vector polarizabilities of both nucleons. As has been shown analytically, the polarizabilities $P^{(01,01)1}$, $P^{(11,11)1}$ and $P^{(11,00)1}$ satisfy the constraints of (21). Moreover, our results fulfill the relations (18)–(20) for arbitrary values of \bar{q} .

The vector polarizabilities of proton and neutron differ significantly in four cases. For $P^{(01,01)1}$ and $P^{(11,00)1}$ this difference is growing as function of Q_0^2 , $P^{(11,02)1}$ and $\hat{P}^{(11,2)1}$ differ for the two nucleons over the whole range of Q_0^2 .

In the following discussion we focus on the proton. Apart from a sign the values of $P^{(01,01)1}$ and $P^{(11,11)1}$ are very similar, even if their behaviour on Q_0^2 is slightly different. It is worthwhile to compare these two polarizabilities to their scalar partners $P^{(01,01)0}$ and $P^{(11,11)0}$ (see the results in ref. [13]), which are proportional to α and β , respectively. While the absolute values of the scalar polarizabilities decrease as function of Q_0^2 , the vector polarizabilities increase. On the other hand, the ratios evaluated at $Q_0^2 = 0.33 \text{ GeV}^2$,

$P_p^{(01,01)0}/P_p^{(01,01)1} \approx -9.4$, $P_p^{(11,11)0}/P_p^{(11,11)1} \approx -7.8$, demonstrate that the scalar polarizabilities α and β will dominate the residual amplitude for the kinematic typical at MAMI. Contrary to this, the remaining scalar polarizability $\hat{P}_p^{(01,1)0}$ is comparable to the vector polarizability $\hat{P}_p^{(01,1)1}$. For increasing Q_0^2 both quantities tend to zero but remain of the same order of magnitude.

Among the 3 polarizabilities $P^{(01,12)1}$, $P^{(11,02)1}$ and $\hat{P}^{(01,1)1}$ with the common unit fm^4 , $P^{(01,12)1}$ is generally suppressed.

Since the polarizabilities have different dimensions due to their definitions (11,12), the amplitudes of (13)–(17) are constructed by multiplying the polarizabilities with different kinematical factors. Therefore, the influence of a particular polarizability can only be seen after evaluating the expansion coefficients (13)–(17).

The LSM and the CQM calculation of Liu et al. [11] predict signs different from ours for two of the vector polarizabilities ($P^{(01,01)1}$, $\hat{P}^{(01,1)1}$). Furthermore, with the exception of $P^{(11,00)1}$, the variation of the vector polarizabilities at low Q_0^2 is much stronger in the LSM than in the CQM, as was the case for the scalar polarizabilities [13]. However, the most remarkable difference between the models is in the absolute values of the vector polarizabilities. Except for $P^{(11,11)1}$ and $P^{(01,12)1}$, our results are substantially larger than the CQM predictions, in the most striking case of $P^{(11,00)1}$ by three orders of magnitude. This result indicates that for most of the vector polarizabilities the nonresonant background, described in our calculation to one-loop, is more important than the nucleon resonances.

The most obvious resonance contribution is due to the strong M1 transition to the $\Delta(1232)$, which leads to the large value of $P^{(11,11)1}$ in the CQM. On the other hand, the CQM violates the model-independent constraint $P^{(11,11)1}(0) = 0$. This shortcoming of the CQM can probably be traced back to the lack of covariance. Similarly, the main contribution to $P^{(01,12)1}$ in the CQM is caused by the $D_{13}(1520)$, which is clearly visible in the photoabsorption spectrum.

B. Contribution of anomaly diagrams

The two anomaly diagrams in Fig. 1 give rise to the amplitude

$$T_a = \frac{e^2 g_{\pi N}^2}{2\pi} \frac{m_N}{t - m_\pi^2} \tau_0 \bar{u}(p') \gamma_5 u(p) \text{Tr}(\gamma_5 \not{\epsilon} \not{q} \not{q}') L_0(t, q^2), \quad (23)$$

$$L_0(t, q^2) = \frac{1}{16\pi^2} \int_0^1 dx \int_0^1 dy \frac{x}{m_N^2 - tx^2y(1-y) - q^2x(1-x)y},$$

with the Mandelstam variable $t = (q - q')^2$. The matrix τ_0 acting in isospace gives opposite signs for proton and neutron. The anomaly contributes to 5 of the 7 vector polarizabilities. In the case of the proton these contributions read

$$P_{p,a}^{(11,00)1}(Q_0^2) = \frac{1}{\sqrt{3}} \frac{\omega_0}{m_N} I(Q_0^2), \quad P_{p,a}^{(11,11)1}(Q_0^2) = \frac{1}{m_N} \frac{\omega_0^2}{\bar{q}^2} I(Q_0^2),$$

$$P_{p,a}^{(01,12)1}(Q_0^2) = \frac{1}{\sqrt{2} m_N^2} \frac{m_N \omega_0}{\bar{q}^2} I(Q_0^2), \quad P_{p,a}^{(11,02)1}(Q_0^2) = -\frac{\sqrt{2}}{\sqrt{3} m_N^2} \frac{m_N \omega_0}{\bar{q}^2} I(Q_0^2),$$

$$\hat{P}_{p,a}^{(01,1)1}(Q_0^2) = -\frac{1}{\sqrt{6}m_N^2} \frac{m_N \omega_0}{\bar{q}^2} I(Q_0^2), \quad (24)$$

$$\text{with } I(Q_0^2) = \frac{g_{\pi N}^2}{6\pi^2 m_N^2} \sqrt{\frac{E+m_N}{2E}} \frac{m_N^2}{m_\pi^2 + Q_0^2} \frac{m_N^2}{\sqrt{4m_N^2 Q_0^2 + Q_0^4}} \ln \frac{2m_N^2 + Q_0^2 + \sqrt{4m_N^2 Q_0^2 + Q_0^4}}{2m_N^2 + Q_0^2 - \sqrt{4m_N^2 Q_0^2 + Q_0^4}},$$

$$\text{and } I(0) = \frac{g_{\pi N}^2}{6\pi^2 m_\pi^2}.$$

In the 3 linear combinations of polarizabilities (structure functions) that can be determined in an unpolarized experiment, the contribution of the anomaly drops out. However, in the case of double polarization experiments the anomaly is very essential. To demonstrate the great importance of the anomaly we have, as an example, plotted the polarizability $\hat{P}_p^{(01,1)1}$ with and without anomaly contribution in Fig. 3.

C. Analytical results

As in the scalar case [13] all vector polarizabilities can be calculated analytically at $Q_0^2 = 0$. Instead of quoting the complete analytical expressions we have given an expansion in powers of the pion mass. Using the definition $\mu = m_\pi/m_N$ we arrive at the following results:

$$\begin{aligned} P_p^{(11,02)1}(0) &= \sqrt{\frac{2}{3}} C \left[\left(\frac{6}{\mu^2} \right) - \frac{1}{2\mu^2} + \frac{3\pi}{8\mu} + 3 \ln \mu + \frac{13}{4} + \mathcal{O}(\mu) \right], \\ P_n^{(11,02)1}(0) &= \sqrt{\frac{2}{3}} C \left[\left(-\frac{6}{\mu^2} \right) - \frac{1}{2\mu^2} - \frac{\pi}{8\mu} + \ln \mu + \frac{3}{4} + \mathcal{O}(\mu) \right], \\ P_p^{(01,12)1}(0) &= \frac{1}{\sqrt{2}} C \left[\left(-\frac{6}{\mu^2} \right) - \frac{1}{2\mu^2} + \frac{7\pi}{8\mu} + 3 \ln \mu - \frac{5}{4} + \mathcal{O}(\mu) \right], \\ P_n^{(01,12)1}(0) &= \frac{1}{\sqrt{2}} C \left[\left(\frac{6}{\mu^2} \right) - \frac{1}{2\mu^2} + \frac{5\pi}{8\mu} + \ln \mu - \frac{1}{4} + \mathcal{O}(\mu) \right], \\ \hat{P}_p^{(01,1)1}(0) &= \frac{1}{\sqrt{6}} C \left[\left(\frac{6}{\mu^2} \right) - \frac{3}{2\mu^2} + \frac{21\pi}{8\mu} + 21 \ln \mu + \frac{85}{4} + \mathcal{O}(\mu) \right], \\ \hat{P}_n^{(01,1)1}(0) &= \frac{1}{\sqrt{6}} C \left[\left(-\frac{6}{\mu^2} \right) - \frac{3}{2\mu^2} + \frac{15\pi}{8\mu} + 7 \ln \mu + \frac{1}{4} + \mathcal{O}(\mu) \right], \\ \hat{P}_p^{(11,2)1}(0) &= \sqrt{\frac{2}{5}} \frac{C}{m_N} \left[-\frac{\pi}{4\mu} - 3 \ln \mu - 4 + \mathcal{O}(\mu) \right], \\ \hat{P}_n^{(11,2)1}(0) &= \sqrt{\frac{2}{5}} \frac{C}{m_N} \left[-\frac{3\pi}{8\mu} - \ln \mu + \frac{1}{4} + \mathcal{O}(\mu) \right], \end{aligned} \quad (25)$$

$$\text{with } C = \frac{g_{\pi N}^2}{72\pi^2 m_N^4}.$$

In eq. (25) the expressions in round brackets denote the contribution of the anomaly. The results confirm that the anomaly diagrams dominate the polarizabilities whenever they contribute. With the exception of $\hat{P}^{(11,2)1}$, the scalar and vector polarizabilities show two common properties: First, the leading terms of the loop contributions do not depend on isospin, and second, the dominant chiral logarithm is three times larger for the proton than for the neutron. However, the scalar and vector polarizabilities differ in their chiral behaviour. Apart from $\hat{P}^{(11,2)1}$, the leading term of the non-vanishing vector polarizabilities is proportional to m_π^{-2} , while the scalar polarizabilities diverge like m_π^{-1} in the chiral limit [13].

By means of eq. (22) one immediately obtains the third order spin-polarizabilities γ_3 and $\gamma_2 + \gamma_4$. The leading order term of our results agrees with a calculation of Bernard et al. [25] who evaluated all 4 spin-polarizabilities for RCS on the basis of heavy baryon chiral perturbation theory (HBChPT) to lowest order ($\mathcal{O}(p^3)$).

The relationship between the LSM and ChPT holds for all vector polarizabilities. A calculation of Hemmert et al. in HBChPT to the order $\mathcal{O}(p^3)$ [18] completely agrees with the leading terms of the chiral expansion (25), except for $\hat{P}^{(11,2)1}$, which vanishes in ChPT to order $\mathcal{O}(p^3)$. Therefore, in ChPT a $\mathcal{O}(p^4)$ calculation is required to obtain the terms in m_π^{-1} .

The agreement between HBChPT and the LSM is restricted to the leading m_π^{-2} term of the chiral expansion. The next to leading order contributions will be modified by various low energy constants which enter a $\mathcal{O}(p^4)$ calculation and describe physics beyond the scope of the sigma model (e.g. resonance contributions, kaon-loops). As an example we refer to the calculation of α and β in RCS to the order $\mathcal{O}(p^4)$ in HBChPT [26].

At $Q_0^2 = 0$, all vector polarizabilities have a finite derivative whose leading terms in the chiral expansion are given in Appendix A. The derivatives of those polarizabilities which vanish at $Q_0^2 = 0$ diverge like m_π^{-2} in the chiral limit, the slope of the remaining polarizabilities is proportional to m_π^{-4} . All analytical results given in App. A satisfy the model-independent relations (18)–(20) between the vector polarizabilities. We stress that we have obtained a complete agreement with the HBChPT calculation to order $\mathcal{O}(p^3)$ [18], also for the first and second derivatives of the polarizabilities.

V. SUMMARY AND CONCLUSION

The non Born amplitude of VCS off the nucleon may be parametrized by 10 generalized polarizabilities, to leading order in the cm energy [2]. To complete our previous calculation [13] we have evaluated the 7 vector polarizabilities which determine the spin-dependent amplitude of the VCS reaction. To this end, we used the LSM in the one-loop approximation and in the limit of an infinite sigma mass. Both our numerical and analytical results are in complete agreement with 3 relations between the vector polarizabilities which have been derived in a model-independent way [10].

We find that the anomaly diagrams strongly affect 5 of the vector polarizabilities. In particular, when measuring double polarization observables like in the proposed reaction $p(\vec{e}, e'\vec{p}')\gamma$ [7], the anomaly contributions become quite important. In the 3 independent

structure functions of the unpolarized cross section, the anomaly contributions cancel exactly.

At $Q_0^2 = 0$, we have performed a Taylor expansion of all polarizabilities (with respect to Q_0^2) keeping the first two non-vanishing coefficients. The various Taylor coefficients have been expanded in powers of m_π and compared with the results of ChPT. It turns out that both calculations totally agree in the leading, isospin-independent term of the chiral expansion [18]. The same is true in the case of the third order spin-polarizabilities γ_3 and $\gamma_2 + \gamma_4$ of real Compton scattering [25]. Of course, a future $\mathcal{O}(p^4)$ calculation in ChPT will give rise to additional low energy constants.

In comparison to the CQM [11] the LSM leads to substantially larger results for 5 of the 7 vector polarizabilities. In the case of $P^{(11,00)1}$ the ratio of the predictions reaches three orders of magnitude. We conclude that most of the vector polarizabilities are dominated by virtual excitations of nonresonant πN scattering states. Only in the case of $P^{(11,11)1}$, the result of the LSM is small compared to the CQM, which is due to the strong influence of the $\Delta(1232)$ resonance on that polarizability. The CQM, however, does not fulfill the model-independent condition $P^{(11,11)1}(0) = 0$.

In conclusion, the generalized vector polarizabilities represent suitable observables to distinguish between different models, and, in particular, to test the chiral structure of the nucleon. Accordingly, experimental effort to measure these quantities is certainly worthwhile, despite the huge difficulties involved in clearly separating the effects of individual polarizabilities.

VI. ACKNOWLEDGEMENT

We would like to thank G. Knöchlein and S. Scherer for several useful discussions. We are also grateful to G. Q. Liu for providing us with the results of the quark model calculation. This work has been supported by the Deutsche Forschungsgemeinschaft (SFB 201).

APPENDIX A: CHIRAL EXPANSION OF THE FIRST AND SECOND DERIVATIVES OF THE POLARIZABILITIES

Below we list the chiral expansion of the first derivatives of the vector polarizabilities. The constant C is defined in equation (25).

$$\begin{aligned}\frac{d}{dQ_0^2}P_p^{(01,01)1}(0) &= \frac{C}{2m_\pi} \left[\frac{1}{\mu} - \frac{17\pi}{8} + \mathcal{O}(\mu) \right], \\ \frac{d}{dQ_0^2}P_n^{(01,01)1}(0) &= \frac{C}{2m_\pi} \left[\frac{1}{\mu} - \frac{9\pi}{8} + \mathcal{O}(\mu) \right], \\ \frac{d}{dQ_0^2}P_p^{(11,11)1}(0) &= \frac{C}{2m_\pi} \left[\left(\frac{6}{\mu} \right) - \frac{1}{2\mu} + \frac{7\pi}{8} + \mathcal{O}(\mu) \right], \\ \frac{d}{dQ_0^2}P_n^{(11,11)1}(0) &= \frac{C}{2m_\pi} \left[\left(-\frac{6}{\mu} \right) - \frac{1}{2\mu} + \frac{5\pi}{8} + \mathcal{O}(\mu) \right],\end{aligned}$$

$$\begin{aligned}
\frac{d}{dQ_0^2} P_p^{(11,00)1}(0) &= \frac{1}{\sqrt{3}} \frac{Cm_N}{2m_\pi} \left[\left(-\frac{12}{\mu}\right) - \frac{5}{\mu} + 12\pi + \mathcal{O}(\mu) \right], \\
\frac{d}{dQ_0^2} P_n^{(11,00)1}(0) &= \frac{1}{\sqrt{3}} \frac{Cm_N}{2m_\pi} \left[\left(\frac{12}{\mu}\right) - \frac{5}{\mu} + 7\pi + \mathcal{O}(\mu) \right], \\
\frac{d}{dQ_0^2} P_p^{(11,02)1}(0) &= \sqrt{\frac{2}{3}} \frac{2Cm_N}{5m_\pi^3} \left[\left(-\frac{15}{\mu}\right) + \frac{1}{4\mu} - \frac{3\pi}{16} + \mathcal{O}(\mu) \right], \\
\frac{d}{dQ_0^2} P_n^{(11,02)1}(0) &= \sqrt{\frac{2}{3}} \frac{2Cm_N}{5m_\pi^3} \left[\left(\frac{15}{\mu}\right) + \frac{1}{4\mu} - \frac{\pi}{16} + \mathcal{O}(\mu) \right], \\
\frac{d}{dQ_0^2} P_p^{(01,12)1}(0) &= \frac{1}{\sqrt{2}} \frac{2Cm_N}{5m_\pi^3} \left[\left(\frac{15}{\mu}\right) + \frac{1}{4\mu} - \frac{9\pi}{32} + \mathcal{O}(\mu) \right], \\
\frac{d}{dQ_0^2} P_n^{(01,12)1}(0) &= \frac{1}{\sqrt{2}} \frac{2Cm_N}{5m_\pi^3} \left[\left(-\frac{15}{\mu}\right) + \frac{1}{4\mu} - \frac{7\pi}{32} + \mathcal{O}(\mu) \right], \\
\frac{d}{dQ_0^2} \hat{P}_p^{(01,1)1}(0) &= \frac{1}{\sqrt{6}} \frac{2Cm_N}{5m_\pi^3} \left[\left(-\frac{15}{\mu}\right) + \frac{1}{2\mu} - \frac{9\pi}{16} + \mathcal{O}(\mu) \right], \\
\frac{d}{dQ_0^2} \hat{P}_n^{(01,1)1}(0) &= \frac{1}{\sqrt{6}} \frac{2Cm_N}{5m_\pi^3} \left[\left(\frac{15}{\mu}\right) + \frac{1}{2\mu} - \frac{7\pi}{16} + \mathcal{O}(\mu) \right], \\
\frac{d}{dQ_0^2} \hat{P}_p^{(11,2)1}(0) &= \sqrt{\frac{2}{5}} \frac{3C}{10m_\pi^3} \left[\frac{1}{12\mu} - \frac{\pi}{32} + \mathcal{O}(\mu) \right], \\
\frac{d}{dQ_0^2} \hat{P}_n^{(11,2)1}(0) &= \sqrt{\frac{2}{5}} \frac{3C}{10m_\pi^3} \left[\frac{1}{12\mu} + \frac{\pi}{32} + \mathcal{O}(\mu) \right]. \tag{A1}
\end{aligned}$$

We also quote the second derivatives of those polarizabilities which vanish at $Q_0^2 = 0$.

$$\begin{aligned}
\frac{d^2}{(dQ_0^2)^2} P_p^{(01,01)1}(0) &= \frac{2C}{5m_\pi^3} \left[-\frac{3}{8\mu} + \frac{15\pi}{32} + \mathcal{O}(\mu) \right], \\
\frac{d^2}{(dQ_0^2)^2} P_n^{(01,01)1}(0) &= \frac{2C}{5m_\pi^3} \left[-\frac{3}{8\mu} + \frac{9\pi}{32} + \mathcal{O}(\mu) \right], \\
\frac{d^2}{(dQ_0^2)^2} P_p^{(11,11)1}(0) &= \frac{2C}{5m_\pi^3} \left[\left(-\frac{15}{\mu}\right) + \frac{1}{8\mu} - \frac{9\pi}{64} + \mathcal{O}(\mu) \right], \\
\frac{d^2}{(dQ_0^2)^2} P_n^{(11,11)1}(0) &= \frac{2C}{5m_\pi^3} \left[\left(\frac{15}{\mu}\right) + \frac{1}{8\mu} - \frac{7\pi}{64} + \mathcal{O}(\mu) \right], \\
\frac{d^2}{(dQ_0^2)^2} P_p^{(11,00)1}(0) &= \frac{1}{\sqrt{3}} \frac{2Cm_N}{5m_\pi^3} \left[\left(\frac{30}{\mu}\right) + \frac{7}{4\mu} - \frac{39\pi}{16} + \mathcal{O}(\mu) \right],
\end{aligned}$$

$$\frac{d^2}{(dQ_0^2)^2} P_n^{(11,00)1}(0) = \frac{1}{\sqrt{3}} \frac{2Cm_N}{5m_\pi^3} \left[\left(-\frac{30}{\mu} \right) + \frac{7}{4\mu} - \frac{25\pi}{16} + \mathcal{O}(\mu) \right]. \quad (\text{A2})$$

REFERENCES

- [1] Proceedings on the workshop VCS96, Ed. V. Breton, Clermont–Ferrand, 1996.
- [2] P.A.M. Guichon, G.Q. Liu and A.W. Thomas, Nucl. Phys. **A591**, 606 (1995).
- [3] G. Audit et al., MAMI proposal on ‘Nucleon structure study by Virtual Compton Scattering’ (1995).
- [4] B. Asavapibhop et al., MIT–Bates proposal on ‘Virtual Compton Scattering on the Proton below Pion Threshold’ (1997).
- [5] G. Audit et al., CEBAF proposal PR–93–050 (1993).
- [6] D. Drechsel, G. Knöchlein, A. Metz and S. Scherer, Phys. Rev. **C55**, 424 (1997).
- [7] M. Vanderhaeghen, to be published in Phys. Lett. **B**.
- [8] M. Vanderhaeghen, D. Lhuillier, D. Marchand and J. Van de Wiele, in preparation.
- [9] H. W. Fearing and S. Scherer, TRIUMF report TRI-PP-96-28, Mainz report MKPH-T-96-18, nucl-th/9607056.
- [10] D. Drechsel, G. Knöchlein, A. Yu. Korchin, A. Metz and S. Scherer, Mainz report MKPH-T-97-11, nucl-th/9704064, submitted to Phys. Rev. **C**.
- [11] G.Q. Liu, A.W. Thomas and P.A.M. Guichon, Austral. J. Phys. **49**, 905 (1996), nucl-th/9605032.
- [12] M. Vanderhaeghen, Phys. Lett. **B368**, 13 (1996).
- [13] A. Metz and D. Drechsel, Z. Phys **A356**, 351 (1996), Mainz–Report MKPH-T-96-8.
- [14] T.R. Hemmert, B.R. Holstein, G. Knöchlein and S. Scherer, Phys. Rev. **D55**, 2630 (1997).
- [15] T.R. Hemmert, B.R. Holstein, G. Knöchlein and S. Scherer, nucl-th/9606051, in Proceedings on the workshop VCS96, Ed. V. Breton, Clermont–Ferrand, 1996.
- [16] Myunggyu Kim and Dong-Pil Min, hep-ph/9704381.
- [17] T.R. Hemmert, B.R. Holstein, G. Knöchlein and S. Scherer, submitted to Phys. Rev. Lett.
- [18] T.R. Hemmert, B.R. Holstein, G. Knöchlein and S. Scherer, in preparation.
- [19] A. Yu. Korchin and O. Scholten, private communication.
- [20] A. Metz and D. Drechsel, nucl-th/9607050, in Proceedings on the workshop VCS96, Ed. V. Breton, Clermont–Ferrand, 1996.
- [21] J.D. Bjorken and S.D. Drell, Relativistic Quantum Mechanics, New York: McGraw–Hill 1964.
- [22] R. Tarrach, Nuovo Cimento **28A**, 409 (1975).
- [23] S. Scherer, A.Yu. Korchin and J.H. Koch, Phys. Rev. **C54**, 904 (1996).
- [24] S. Ragusa, Phys. Rev. **D47**, 3757 (1993); Phys. Rev. **D49**, 3157 (1994).
- [25] V. Bernard, N. Kaiser and U.G. Meißner, Int. J. Mod. Phys. **E4**, 193 (1995).
- [26] V. Bernard, N. Kaiser, U.G. Meißner and A. Schmidt, Phys. Lett. **B319**, 269 (1993); Z. Phys. **A348**, 317 (1994).

FIGURES

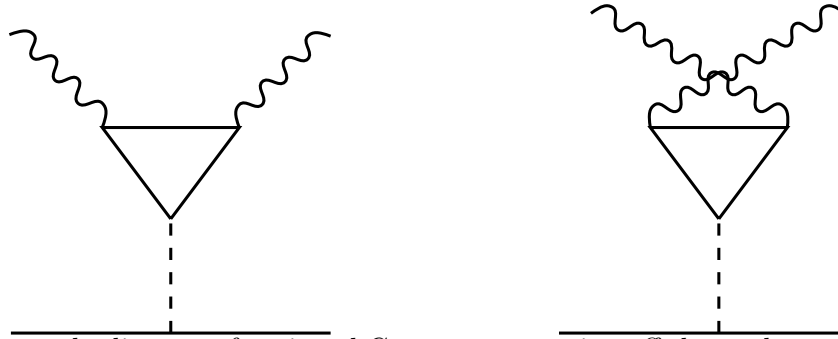
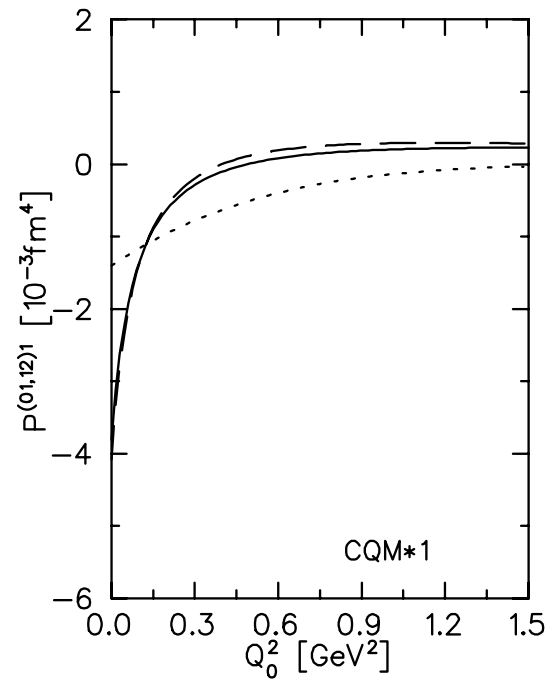
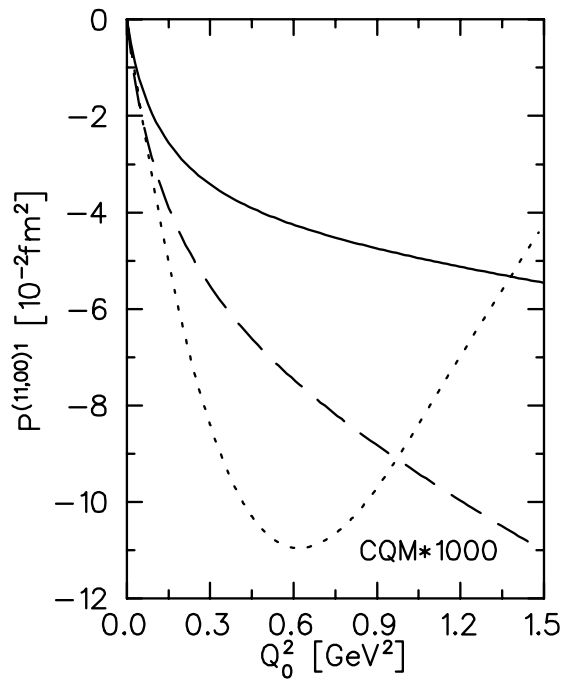
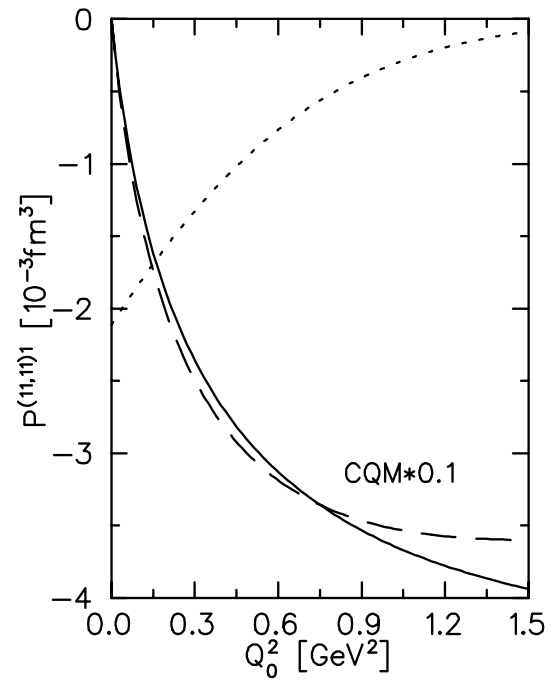
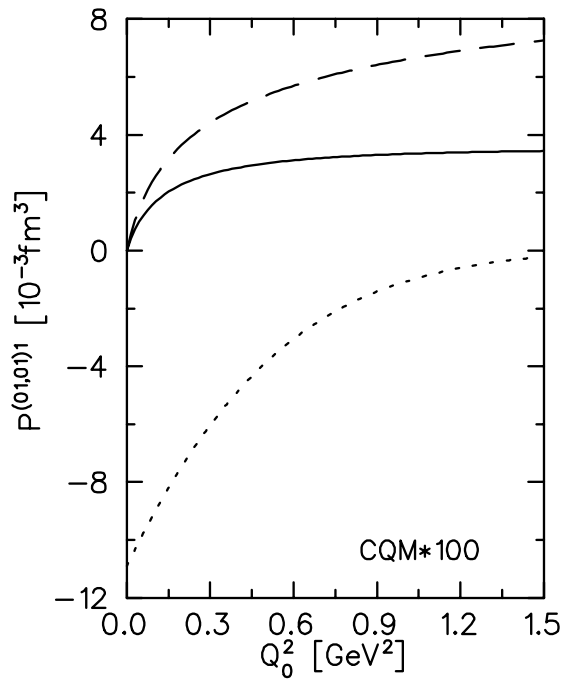


FIG. 1. Anomaly diagrams for virtual Compton scattering off the nucleon. Solid lines: nucleons, wavy lines: photons, dotted lines: neutral pions.



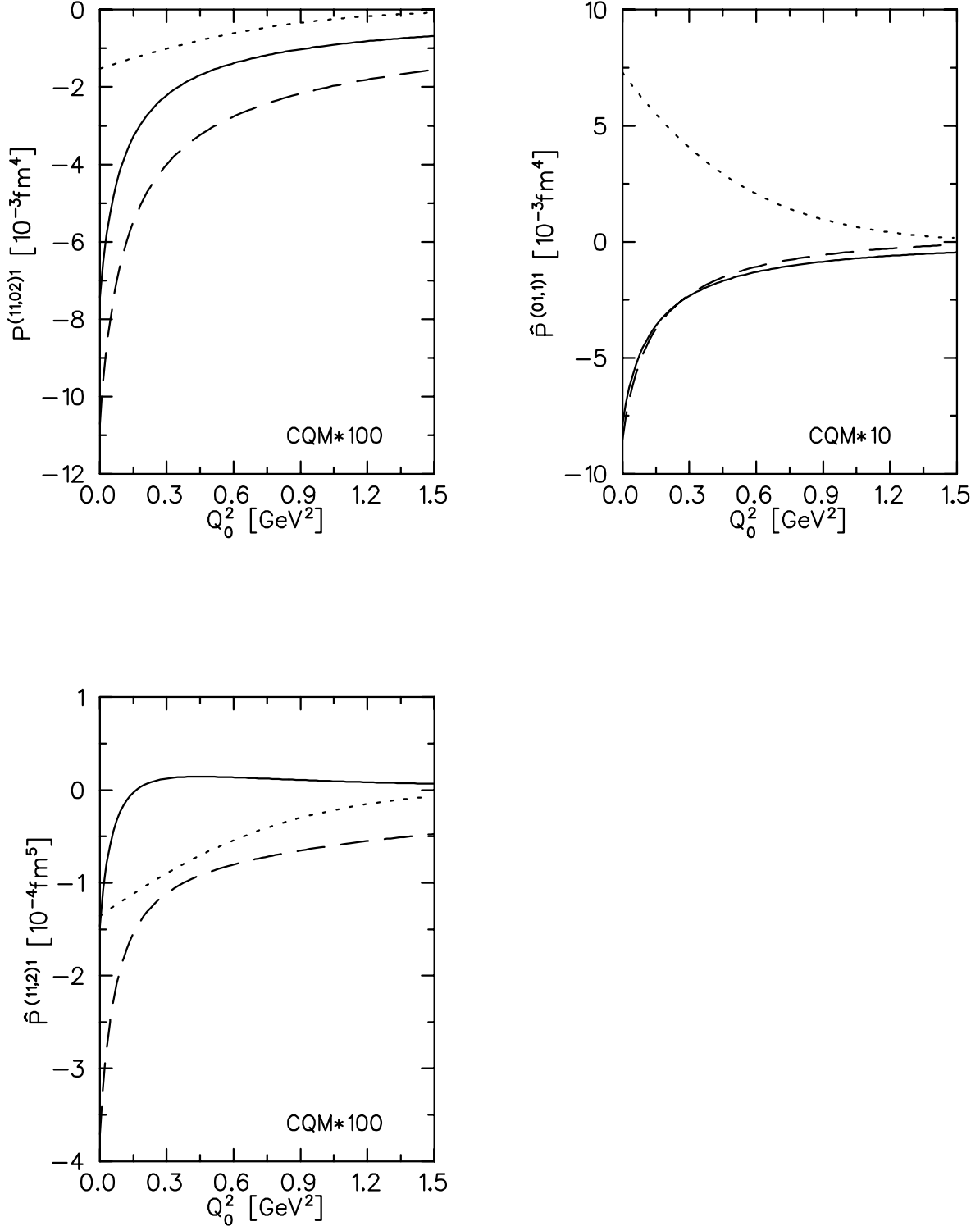


FIG. 2. The vector polarizabilities as functions of momentum transfer. Solid line: calculation with the LSM for the proton, dashed line: LSM result for the neutron, dash-dotted line: CQM for the proton [11]. Note that the CQM results have been scaled.

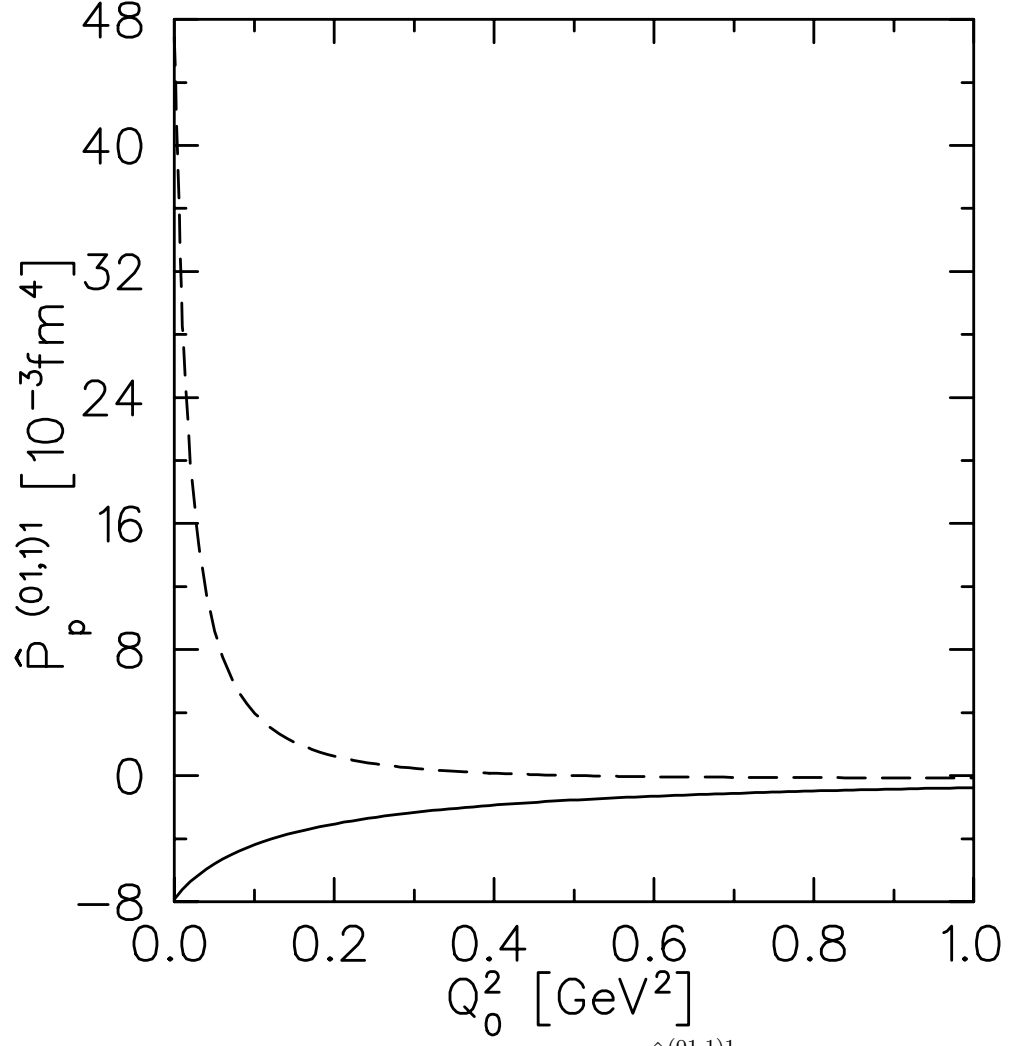


FIG. 3. Influence of the anomaly on the polarizability $\hat{P}_p^{(01,1)1}$. Solid line: without anomaly, dashed line: anomaly included.